Synthesis of Nanoporous Carbon from Ulva Lactuca Activated by Eggshell for CO2 Capture: A Novel Approach to Waste Valorization

Khadija MAMMADYAROVA
Yildiz Teknik Universitesi
Müge Sarı YILMAZ
mugesari@yildiz.edu.tr

Yildiz Teknik Universitesi Kimya Metalurji Fakultesi

Research Article

Keywords: Nanoporous carbons, CO2 adsorption, algae, eggshells, waste recycling

Posted Date: July 1st, 2024

DOI: https://doi.org/10.21203/rs.3.rs-4417833/v1

Version of Record: A version of this preprint was published at Environmental Science and Pollution Research on October 4th, 2024. See the published version at https://doi.org/10.1007/s11356-024-35101-z.

Abstract

Facing the daunting challenge of climate change, driven by escalating greenhouse gas concentrations, our research introduces an innovative solution for CO_2 capture. We explore a novel nanoporous carbon derived from Ulva Lactuca, activated with eggshell waste, spotlighting waste valorization in mitigating atmospheric CO_2. Through a systematic methodology encompassing variable carbonization temperatures (700–900°C) and nitrogen flow rates (2–4 ml/min), complemented by a suite of characterization techniques, we unveil the synthesis of this pioneering adsorbent. Our study not only presents a novel, sustainable pathway for CO_2 capture but also demonstrates superior performance, particularly with the NC800-4 sample, achieving a CO_2 capture capacity of 1.40 mmol/g at 30°C, alongside demonstrating consistent adsorption efficiency over four successive adsorption/desorption cycles. This breakthrough underscores the potential of leveraging waste for environmental remediation, offering a dual solution to waste management and CCUS applications.

INTRODUCTION

The growth of industry and the ever-increasing demand for energy have increased the use of fossil fuels. The combustion process during fossil fuel use is responsible for most of the greenhouse gas emissions, and the increase in the amount of these gases, especially carbon dioxide (CO_2), accelerates global warming and causes climate change (Kumar, 2018). Natural disasters show how critical this situation is becoming more and more evident every day. In order to achieve the necessary goals and targets, it is not enough to reduce future CO_2 emissions, but the CO_2 currently in the atmosphere must be captured and stored by different methods (World Energy Outlook 2022, n.d.). Decarbonization of industry and industrial systems is also an urgent challenge for "hard-to-decarbonize" industries such as steel, cement, and chemical production. Carbon capture, utilization, and storage systems need to be developed to address this immense challenge.

Methods such as absorption, physical adsorption, chemical adsorption, membrane separation methods, and cryogenic combustion are employed to capture or reduce CO_2 emissions in the atmosphere. Currently, the most widely utilized industrial-scale method for CO_2 capture is amine-based absorption. However, this method has disadvantages such as high energy consumption, loss of function of the material used over time, corrosion of the devices and vaporization of the material during the regeneration process (Yuan et al., 2019). Additional methods for eliminating emissions in the atmosphere include direct air capture (DAC), bioenergy carbon capture and storage (BECCS), afforestation, and reforestation which are collectively referred to as negative carbon methods (McLaughlin et al., 2023). Recent studies have shown that adsorption using biomaterial-based solid and nanoporous materials is both environmentally friendly and energy efficient. Moreover, these materials are highly appealing due to their low cost and high CO_2 capture capacity. Researchers are mindful of selecting biomaterials that are available as waste, making them useful for waste management purposes

(Montalvão et al., 2016). These materials can be used for both carbon capture and direct removal of carbon from the atmosphere (Rehman & Park, 2019).

Nanoporous carbon materials are known for their impressive physicochemical properties, making them widely used for various applications. They are particularly noted for their excellent properties in adsorption and high selectivity towards various adsorbates (Heidari et al., 2014). However, for large-scale application of these materials, it is necessary to develop a simple, efficient and economical production process. In this way, it will be advantageous to use an efficient nanoporous carbon-based adsorbent based on biomass to be practically used in air pollution control, capture, removal and storage of greenhouse gases and recovery of volatile organic chemicals (Memetova et al., 2022).

Algal biomass, another waste product, is also utilized in the production of carbon-based materials. They are classified as macroalgae or microalgae according to their size. They typically grow in fresh and salty waters, as well as on wet soils, rocks, and trees (Gilmour, 2023). Marine macroalgae, commonly known as seaweeds, are multicellular photoautotrophic organisms that require light, nutrients and CO_2 dissolved in water to survive (Weier et al., 1970). Ulva Lactuca (U. Lactuca), also known as "sea lettuce," is an edible macroalgae species. U. Lactuca macroalgae acts as a high nutrient reservoir for other harmful species, providing a basis for the increase of toxic species and leading to the deterioration of the marine ecosystem (Ozyigit et al., 2017; Tang & Gobler, 2011). This species, which grows in large quantities, can also cause disadvantages in human life by accumulating on beaches, seashores, canals and stream mouths and creating physical difficulties (Zingone et al., 2021).

The literature review reveals that different organic wastes and plants have been used in the synthesis of nanoporous carbon. Although natural resources were utilized in these studies, materials were activated by using KOH, which is generally harmful, expensive and corrosive for the environment, to increase the CO_2 capture performance of the materials(de Souza et al., 2020; Huang et al., 2019; Lillo-Ródenas et al., 2004; Serafın et al., 2022). In this context, the study aims to activate the surface of macroalgae wastes by using eggshell wastes as an alternative to KOH.

Eggshells, which will be used as activating agent within the scope of the study, are in the hazardous waste category according to European Union regulations (Laca et al., 2017). These wastes typically create a microbial environment and lead to the release of odor and toxic gases. Additionally, global egg production is predicted to reach 86.8 million tons by 2030, according to statistics from the Food and Agriculture Organization (FAO) (Zaheer, 2015). Global demand and production for eggs have increased steadily since the turn of the century. In 2018, 76.7 million tons of eggs were produced worldwide, an increase of 14.95% compared to the previous decade (Aditya et al., 2021). Therefore, creating a new use for this waste and bringing it into the economy will make a significant contribution to the management of waste.

In this study, novel nanoporous carbon was synthesized from U. Lactuca macroalgae surface activated with eggshell. By applying different carbonization temperatures and different gas flow rates, the CO_2

capture capacities of each carbon at different temperatures were examined for the first time. According to the analysis results, sequential adsorption/desorption cycle analysis of the sample with the best capacity was performed and the CO_2 capture efficiency after cycling was determined.

EXPERIMENTAL PROCEDURES

2.1 Materials

The eggshells were collected from household waste. Initially, the eggshells were brushed under running water to remove dirt and dust, then the membrane linings within the shell structure were cleaned using tweezers. The cleaned eggshells, dried at 105°C for 24 hours, were ground in a mechanical grinder and sieved to a size finer than 90 mesh. The obtained eggshell powder was then calcined in a calcination furnace at 950°C for 1 hour. The purpose of calcining eggshells is to completely convert the calcium carbonate ($CaCO_3$) in the shell structure to calcium oxide (CaO). Consequently, the basic calcium hydroxide ($Ca(OH)_2$) necessary for the activation of the macroalgae will be obtained according to the reaction given below with the CaO in the calcined shell reacting with water.

$CaO + H_2O \rightarrow Ca(OH)_2$ (1)

The other raw material, U. Lactuca, was collected from the Kadıköy coast of Istanbul in September. The collected macroalgae were washed under running water to remove impurities such as sand, garbage and bags. They were then dried in an oven at 105°C overnight and ground.

2.2 Characterization

The crystallographic phase properties of the products were obtained by Panalytical X'Pert PRO brand XRD device. XRD analysis of the samples was recorded at diffraction angles ranging from 10–60°. The functional bond groups of the prepared nanoporous carbon materials were analyzed by Fourier transform infrared (FTIR) spectroscopy using Perkin Elmer Spectrum One with Attenuated Total Reflection (ATR) accessory. The textural properties of the prepared carbon samples was characterized by N_2 adsorption/desorption isotherms at 77 K in a Quantachrome (Autorosorb QI model) surface area and pore size analyser. In order to determine the pore structures of the samples, DFT (Density Functional Theory) method was applied. Samples were processed under vacuum at 300°C for 3 hours and made ready for analysis. The surface area (S_{BET}) of the samples has been calculated using the BET equation in the relative pressure range of $P/P_0 = 0.03–0.2$. Total pore volumes (V_{tot}) have been calculated from the amount of nitrogen adsorbed. The micropore volume (V_{micro}) was determined using the N_2 sorption method and quantified by the DFT method. Raman spectroscopy was used to determine the carbon framework structures of the prepared carbon materials. The Raman spectra of the samples were analysed with Perkin Elmer Raman Station 400F model Raman spectroscopy. The morphological properties of the obtained products were examined using the Thermo Scientific Apreo 2 S LoVac Field

Emission Scanning Electron Microscopy (FE-SEM) device. The microstructural properties of the prepared carbon products were determined using an FEI TALOS brand F200S model Transmission Electron Microscopy (TEM) microscope operating at a voltage of 200 kV.

2.3 CO Adsorption Measurement

The CO_2 capture performances of carbon materials at various temperatures (30°C, 75°C, and 100°C) were determined using a Perkin Elmer Pyris Diamond Differential Thermal Analysis/Thermogravimetry Device (DTA/TG) device. Initially, the moisture present in the structure of the predetermined quantity of samples was removed at 105°C under a nitrogen atmosphere. Subsequently, the sample was brought to the desired temperature at a cooling rate of 10°C/min, and the gas flow was switched to a high-purity (99.99%) CO_2 atmosphere and held for a set period. The CO_2 capture capacities of the prepared carbons were ascertained based on the increase in weight of the sample. Additionally, the adsorption/desorption cycle of the nanoporous carbon will be conducted at the temperature where it exhibits the highest capacity, using the same device.

2.4 Synthesis of Activated Carbons From Biomass

Activated carbons from biomass was prepared according to previous study with some modifications (Serafin et al., 2022). Accordingly, U. Lactuca macroalgae and calcined eggshells were weighed in a 1:1 ratio and mixed in a certain amount of distilled water at room temperature. The saturated solution obtained was dried in an oven at 200°C for 18 hours. At the end of the time, the mixture obtained was taken into the tube furnace and carbonized under nitrogen flow at the desired flow rate for 2 hours at the desired temperature. After cooling to room temperature, the sample was washed with distilled water to remove undesired compounds in the process, then filtered and dried. After drying, the sample was treated with 2 M HCl for 1 hour of stirring. It was then allowed to rest for 18 hours at room temperature. At the end of the time, the sample was washed with distilled water and dried at 200°C for 18 hours in order to completely remove the chlorite ion.

Carbonization was carried out at different temperatures (700°C, 800°C, and 900°C) and different flow rates (2 ml/min, 3 ml/min, and 4 ml/min) in order to observe the effect of carbonization temperature and nitrogen flow rate on the structural properties and CO_2 adsorption capacities of the sample. These samples were named as NCX-Y. Here NC stands for nanoporous carbon, X for pyrolysis temperature and Y for nitrogen flow rate. For example, NC700-2 is the sample carbonized at 700°C with a N_2 flow of 2 ml/min.

RESULTS AND DISCUSSION

3.1 Characterisation of Activated Carbons

XRD patterns of nanoporous carbon samples prepared at different temperatures and flow rates are given in Figure 1. No crystalline peaks were detected in the XRD graphs of all samples, indicating that $Ca(OH)_2$ was completely removed from the structure. Additionally, a broad diffraction peak in the range of 20° to 30° and another less intense diffraction peak extending between 40° and 50° were observed in all samples XRD patterns. These two broad diffraction peaks are generally attributed to the graphite crystal planes of activated carbon in the low angle region ((002) graphite peak) and the radial spreading of the crystal structures in the high angle region ((100) graphite peak) (Zhao et al., 2009). As a result, all carbon samples prepared at different temperatures and flow rates were found to be in the form of irregular graphite.

The ATR-FTIR spectra of the prepared carbon samples are presented in Figure 2. According to this, it has been observed that the spectra of the samples are similar. The band around 1028 cm^{-1} originates from C-O stretching vibrations, while the band observed at 1544 cm^{-1} is due to vibrations in the aromatic group (C=C) (Doğan et al., 2020).

Table 1 lists the textural properties of the obtained carbon samples. According to this, as the S_{BET} values of the samples increase, an increase in V_{tot} and V_{micro} values was observed. Additionally, it has been noticed that samples carbonized at 800°C have higher S_{BET}, V_{tot}, and V_{micro} values compared to those carbonized at other temperatures under the same gas flow rates. Furthermore, upon examining samples carbonized at the same temperature but different flow rates, it has been generally observed that an increase in gas flow results in higher S_{BET}, V_{tot}, and V_{micro} values. According to N_2 adsorption/desorption and DFT analyses, the highest S_{BET} (860.83 m^2/g), V_{tot} (1.07 cm^3/g), and V_{micro} (0.99 cm^3/g) values were observed in the NC800-4 sample. The closeness of V_{tot} and V_{micro} values and the low V_{mezo} values indicate that most of the pores in the samples are micropores (Serafin & Dziejarski, 2023; Thommes et al., 2015).

Figure 3 presents the adsorption-desorption isotherms of nitrogen on activated carbons produced from U. lactuca, which were carbonized under different nitrogen flows and temperatures. According to IUPAC classification, the nitrogen physisorption isotherms at 77K for these activated carbons are classified as Type IVa, a behavior typical of mesoporous materials (Thommes et al., 2015). This classification is indicative of capillary condensation occurring within the pores—a process where a gas transforms into a liquid-like phase inside a pore at a pressure (p) that is below the saturation pressure (p_o) of the bulk liquid.

The shape of the hysteresis loop can provide information about the pore structure and connectivity within the material. The hysteresis is the area between the adsorption and desorption curves, and it is an indication of the phenomenon of capillary condensation in the pores. Here, the adsorption is not immediately reversible, leading to the hysteresis effect. Loops typically open where capillary condensation begins and close at the point of capillary evaporation.

The hysteresis loops in the isotherms resemble Type H4 according to the IUPAC classification. The Type H4 hysteresis loop is typically found in materials with slit-shaped pores, often associated with materials that have layered structures. These loops are characterized by almost parallel adsorption and desorption branches and are often typical for micro-mesoporous carbons.

The pore size distribution graphs of the samples, determined using the DFT method, are presented in Figure 4. It is observed that all samples have a sharp peak in the 3-10 Å pore size range and relatively weak peaks in the 10-80 Å range. This suggests that most of the pores in the samples are micropores, and they also possess mesopores. Thus, it has been proven that all the prepared carbon samples are nanoporous (Sing, 1985).

The Raman spectra of nanoporous carbons are displayed in Figure 5. It has been observed that all samples exhibit two characteristic peaks, known as the D and G bands, appearing respectively around 1335 cm^{-1} and 1595 cm^{-1}. The D band is associated with the vibrations of disordered sp3 carbons, while the G band is attributed to the regular sp2 carbon vibrations, representing the crystallinity of the samples (Ferrari & Robertson, 2000). The intensity ratio of the G and D bands (I_G/I_D) is used to determine the regularity of the carbon structures (Serafin et al., 2022).

Table 2 provides the D and G band regions and the I_G/I_D ratios of the samples. It has been found that all prepared nanoporous carbon samples have I_G/I_D values very close to each other, ranging between 0.94 and 0.98. The I_G/I_D ratios of all values are less than 1, which proves the high irregularity in the structure of the obtained materials. The results of the Raman spectroscopy analysis of the nanoporous carbon samples have confirmed the results of the XRD studies.

FE-SEM images of the U. Lactuca and eggshell mixture prepared to observe the change in structure with carbonization are given in Figure 6. According to the images at different magnifications, no pores were observed in the structure of the sample prepared before carbonization.

Figure 7 shows the FE-SEM and TEM images of the prepared carbon samples. When the FE-SEM images of the samples at different magnifications are examined, macro and microporous morphologies are observed in the samples in accordance with the literature. In other words, it is clearly observed that the prepared carbon samples show a porous structure with different pore sizes and shapes compared to the raw material. The pores of the samples are mostly irregular; however, circular and oval shaped pores are also present. According to high magnification TEM images, it was observed that the samples contained significant amounts of small-sized nanopores. The pore morphology observed by FE-SEM and TEM is in accordance with the data obtained from N_2 adsorption/desorption analysis.

3.2 CO_2 Adsorption

The determined CO_2 adsorption capacities of the samples are provided in Table 3. According to the adsorption analysis results at different temperatures, it has been observed that the CO_2 adsorption

capacities of the samples decrease with an increase in temperature. This indicates that CO_2 adsorption occurs through physisorption rather than chemisorption (Sari Yilmaz, 2017). Furthermore, among the samples prepared at different carbonization temperatures, it has been seen that the samples with a flow rate of 2 ml/min have the lowest CO_2 capture capacity at all adsorption temperatures. The highest CO_2 adsorption capacity among the prepared nanoporous carbon samples was observed in the NC800-4 sample. Additionally, it has been found that the CO_2 adsorption capacities increase with the increase in S_{BET}, V_{tot}, and V_{micro} values for samples prepared at the same temperature but different flow rates.

Figure 8 shows the time variation of CO_2 capture capacities at 30°C of carbon samples prepared at different carbonization temperatures and gas flow rates. According to this, the CO_2 adsorption of the samples generally increased rapidly in the first 30 minutes and then slowly and remained constant after 70 minutes.

The CO_2 capture capacities of some porous carbon materials determined with similar conditions in the literature were compared with the highest capture capacity value obtained within the study. It was seen that the NC800-4 sample has the best CO_2 capture capacity among the porous carbons given in Table 4. Therefore, it is concluded that the adsorbent prepared from waste in the present study will be a promising new carbon material for CO_2 capture studies on solid surface.

The regeneration capacity and cyclic stability of the solid adsorbent are important properties for CO_2 sequestering materials. For this purpose, the adsorption/desorption cycle of NC800-4, which has the highest CO_2 capture performance, was investigated isothermally in DTA/TG device at 30°C where it showed the highest capacity. Figure 9 shows four consecutive CO_2 adsorption/desorption cycles and adsorption capacities of the sample at 30°C. Accordingly, the sample exhibits good stability over four consecutive cycles without any significant degradation in adsorption capacity.

CONCLUSION

This study has successfully demonstrated the potential of utilizing U. lactuca macroalgae and eggshell waste as precursors for producing nanoporous carbon materials that are optimized for CO_2 capture. By using eggshells as activators in the preparation of nanoporous carbons, an alternative material to the harmful, expensive, and corrosive activator KOH has been developed. The carbonization temperature and nitrogen flow rate were found to significantly affect the textural properties and CO_2 capture capacities of the sample. The optimized carbon sample (NC800-4) exhibited good regenerability and cyclic stability, highlighting its practical applicability in CO_2 capture efforts.

As a result, this study not only contributes to the growing field of sustainable material science by creating value-added products from waste, but also introduces a promising, cost-effective, and efficient material for reducing CO_2 emissions. The results obtained from this comprehensive analysis pave the

way for future research aimed at optimizing these materials for broader environmental applications, thus contributing to the global effort to combat climate change.

Declarations

Ethical Approval

This is not applicable.

Consent to Participate

All authors consent to participate.

Consent to Publish

All authors consent to publish.

Competing interests

The authors declare that they have no known competing financial interests or personal relationships that could have appeared to influence the work reported in this paper.

Funding

This work was supported by the “Scientific and Technological Research Council of Turkey (TUBITAK) (Project Number: 123M071).

Authors Contributions

Khadija Mammadyarova: Methodology, Investigation, Writing Original Draft. Muge Sari Yilmaz: Methodology, Formal Analysis, Supervision, Conceptualization, Review-Editing. All authors read and approved the final manuscript.

ACKNOWLEDGMENT

We sincerely appreciate the financial assistance received from the Scientific and Technological Research Council of Turkey (TUBITAK) (Project Number: 123M071).

References

1. Aditya S, Stephen J, Radhakrishnan M (2021) Utilization of eggshell waste in calcium-fortified foods and other industrial applications: A review. Trends Food Sci Technol 115:422–432. https://doi.org/10.1016/J.TIFS.2021.06.047
2. de Souza LKC, Gonçalves AAS, Queiroz LS, Chaar JS, da Rocha Filho GN (2020) Utilization of acai stone biomass for the sustainable production of nanoporous carbon for CO2 capture. Sustainable Mater Technol 25 & da Costa, C. E. F. https://doi.org/10.1016/j.susmat.2020.e00168
3. Doğan M, Sabaz P, Bïcïl Z, Koçer Kizilduman B, Turhan Y (2020) Activated carbon synthesis from tangerine peel and its use in hydrogen storage. J Energy Inst 93(6):2176–2185. https://doi.org/10.1016/j.joei.2020.05.011
4. Ferrari A, Robertson J (2000) Interpretation of Raman spectra of disordered and amorphous carbon. Phys Rev B - Condens Matter Mater Phys 61(20):14095–14107. https://doi.org/10.1103/PHYSREVB.61.14095
5. Gilmour DJ (2023) Diversity of algae and their biotechnological potential. Adv Microb Physiol 82:301–321. https://doi.org/10.1016/BS.AMPBS.2023.02.001
6. Heidari A, Younesi H, Rashidi A, Ghoreyshi AA (2014) Adsorptive removal of CO2 on highly microporous activated carbons prepared from Eucalyptus camaldulensis wood: Effect of chemical activation. J Taiwan Inst Chem Eng 45(2):579–588. https://doi.org/10.1016/j.jtice.2013.06.007
7. Huang GG, Liu YF, Wu XX, Cai JJ (2019) Activated carbons prepared by the KOH activation of a hydrochar from garlic peel and their CO2 adsorption performance. Xinxing Tan Cailiao/New Carbon Mater 34(3):247–257. https://doi.org/10.1016/S1872-5805(19)60014-4
8. Kumar A (2018) Global Warming, Climate Change and Greenhouse Gas Mitigation. In Biofuels: Greenhouse Gas Mitigation and Global Warming (pp. 1–16). Springer India. https://doi.org/10.1007/978-81-322-3763-1_1
9. Laca A, Laca A, Díaz M (2017) Eggshell waste as catalyst: A review. In Journal of Environmental Management (Vol. 197, pp. 351–359). Academic Press. https://doi.org/10.1016/j.jenvman.2017.03.088
10. Lillo-Ródenas MA, Juan-Juan J, Cazorla-Amorós D, Linares-Solano A (2004) About reactions occurring during chemical activation with hydroxides. Carbon 42(7):1371–1375. https://doi.org/10.1016/j.carbon.2004.01.008
11. McLaughlin H, Littlefield AA, Menefee M, Kinzer A, Hull T, Sovacool BK, Bazilian MD, Kim J, Griffiths S (2023) Carbon capture utilization and storage in review: Sociotechnical implications for a carbon reliant world. In Renewable and Sustainable Energy Reviews (Vol. 177). Elsevier Ltd. https://doi.org/c
12. Memetova A, Tyagi I, Singh L, Karri RR, Suhas, Tyagi K, Kumar V, Memetov N, Zelenin A, Tkachev A, Bogoslovskiy V, Shigabaeva G, Galunin E, Mubarak NM, Agarwal S (2022) Nanoporous carbon materials as a sustainable alternative for the remediation of toxic impurities and environmental contaminants: A review. In Science of the Total Environment (Vol. 838). Elsevier B.V. https://doi.org/10.1016/j.scitotenv.2022.155943

13. Montalvão S, Demirel Z, Devi P, Lombardi V, Hongisto V, Perälä M, Hattara J, Imamoglu E, Tilvi SS, Turan G, Dalay MC, Tammela P (2016) Large-scale bioprospecting of cyanobacteria, micro- and macroalgae from the Aegean Sea. New Biotechnol 33(3):399–406. https://doi.org/10.1016/j.nbt.2016.02.002
14. Ozyigit II, Uyanik OL, Sahin NR, Yalcin IE, Demir G (2017) Monitoring the pollution level in Istanbul coast of the sea of Marmara using algal species Ulva lactuca L. Pol J Environ Stud 26(2):773–778. https://doi.org/10.15244/pjoes/66177
15. Rehman A, Park SJ (2019) Tunable nitrogen-doped microporous carbons: Delineating the role of optimum pore size for enhanced CO2 adsorption. Chem Eng J 362:731–742. https://doi.org/10.1016/J.CEJ.2019.01.063
16. Sari Yilmaz M (2017) Synthesis of novel amine modified hollow mesoporous silica@Mg-Al layered double hydroxide composite and its application in CO2 adsorption. Microporous Mesoporous Mater 245:109–117. https://doi.org/10.1016/j.micromeso.2017.02.077
17. Serafin J, Dziejarski B (2023) Application of isotherms models and error functions in activated carbon CO2 sorption processes. Microporous Mesoporous Mater 354:112513. https://doi.org/10.1016/J.MICROMESO.2023.112513
18. Serafin J, Kiełbasa K, Michalkiewicz B (2022) The new tailored nanoporous carbons from the common polypody (Polypodium vulgare): The role of textural properties for enhanced CO2 adsorption. Chem Eng J 429. https://doi.org/10.1016/j.cej.2021.131751
19. Sing KSW (1985) Pure Appl Chem 57(4):603–619. https://doi.org/10.1351/pac198557040603. Reporting physisorption data for gas/solid systems with special reference to the determination of surface area and porosity (Recommendations 1984
20. Tang YZ, Gobler CJ (2011) The green macroalga, Ulva lactuca, inhibits the growth of seven common harmful algal bloom species via allelopathy. Harmful Algae 10(5):480–488. https://doi.org/10.1016/j.hal.2011.03.003
21. Thommes M, Kaneko K, Neimark AV, Olivier JP, Rodriguez-Reinoso F, Rouquerol J, Sing KSW (2015) Physisorption of gases, with special reference to the evaluation of surface area and pore size distribution (IUPAC Technical Report). Pure and Applied Chemistry, 87(9–10), 1051–1069. https://doi.org/10.1515/pac-2014-1117
22. Weier TE, Stocking CR, Barbour MG (1970) Botany. An introduction to plant biology
23. World Energy Outlook (2022) (n.d.). .org/t&c/
24. Yuan H, Chen J, Li D, Chen H, Chen Y (2019) 5 Ultramicropore-rich renewable porous carbon from biomass tar with excellent adsorption capacity and selectivity for CO2 capture. Chem Eng J 373:171–178. https://doi.org/10.1016/J.CEJ.2019.04.206
25. Zaheer K (2015) An Updated Review on Chicken Eggs: Production, Consumption, Management Aspects and Nutritional Benefits to Human Health. Food Nutr Sci 06(13):1208–1220. https://doi.org/10.4236/fns.2015.613127

26. Zhao J, Yang L, Li F, Yu R, Jin C (2009) Structural evolution in the graphitization process of activated carbon by high-pressure sintering. Carbon 47(3):744–751. https://doi.org/10.1016/j.carbon.2008.11.006
27. Zingone A, Escalera L, Aligizaki K, Fernández-Tejedor M, Ismael A, Montresor M, Mozetič P, Taş S, Totti C (2021) Toxic marine microalgae and noxious blooms in the Mediterranean Sea: A contribution to the Global HAB Status Report. Harmful Algae 102. https://doi.org/10.1016/j.hal.2020.101843

Tables

Table 1. Textural properties of nanoporous carbons obtained from U. lactuca

Sample	S_{BET} (m^2/g)	V_{tot} (cm^3/g)	V_{mikro} (cm^3/g)	V_{meso} (cm^3/g)
NC700-2	347.936	0.363	0.337	0.026
NC700-3	537.041	0.7410	0.670	0.071
NC700-4	516.737	0. 712	0.645	0.067
NC800-2	573.635	0.719	0.637	0.082
NC800-3	727.081	0.881	0.813	0.068
NC800-4	860.830	1.067	0.986	0.081
NC900-2	375.425	0.450	0.416	0.034
NC900-3	515.6581	0.692	0.616	0.076
NC900-4	611.032	0.910	0.810	0.100

Table 2. D and G band properties of samples according to Raman spectrum

Sample	Positions of D and G bands (cm^{-1})		I_G/I_D
NC700-2	1338	1593	0.96
NC700-3	1338	1599	0.95
NC700-4	1332	1595	0.94
NC800-2	1334	1600	0.96
NC800-3	1338	1600	0.98
NC800-4	1339	1599	0.98
NC900-2	1338	1595	0.95
NC900-3	1336	1598	0.94
NC900-4	1338	1597	0.98

Table 3. CO_2 adsorption capacities of nanoporous carbons

Sample	30 °C	75 °C	100 °C
NC700-2	0.75	0.21	0.12
NC700-3	1.08	0.31	0.18
NC700-4	0.86	0.38	0.25
NC800-2	1.18	0.31	0.16
NC800-3	1.40	0.46	0.25
NC800-4	1.19	0.41	0.29
NC900-2	0.58	0.12	0.02
NC900-3	0.82	0.23	0.12
NC900-4	1.20	0.25	0.08

Table 4. CO_2 capture capacities of some porous carbons reported in the literature

Sample	T (°C)	P (bar)	Capacity ($mmol.g^{-1}$)	Reference
Porous carbon	30	1	0.68	[28]
Porous carbon derived from melamine-formaldehyde	30	1	0.93	[29]
Mesoporous carbon	30	1	0.83	[30]
Ordered mesoporous carbon	30	0.9	0.97	[31]
Nanoporous carbon derived from PET waste	30	1	1.31	[32]
Nitrogen-enriched nanostructured carbon	30	1	0.79	[33]
Nanoporous carbon	0	1	0.90	[34]
Carbon from PET/carbazole	25	1	1.09	[35]
NC800-4	30	1	1.40	This study

Figures

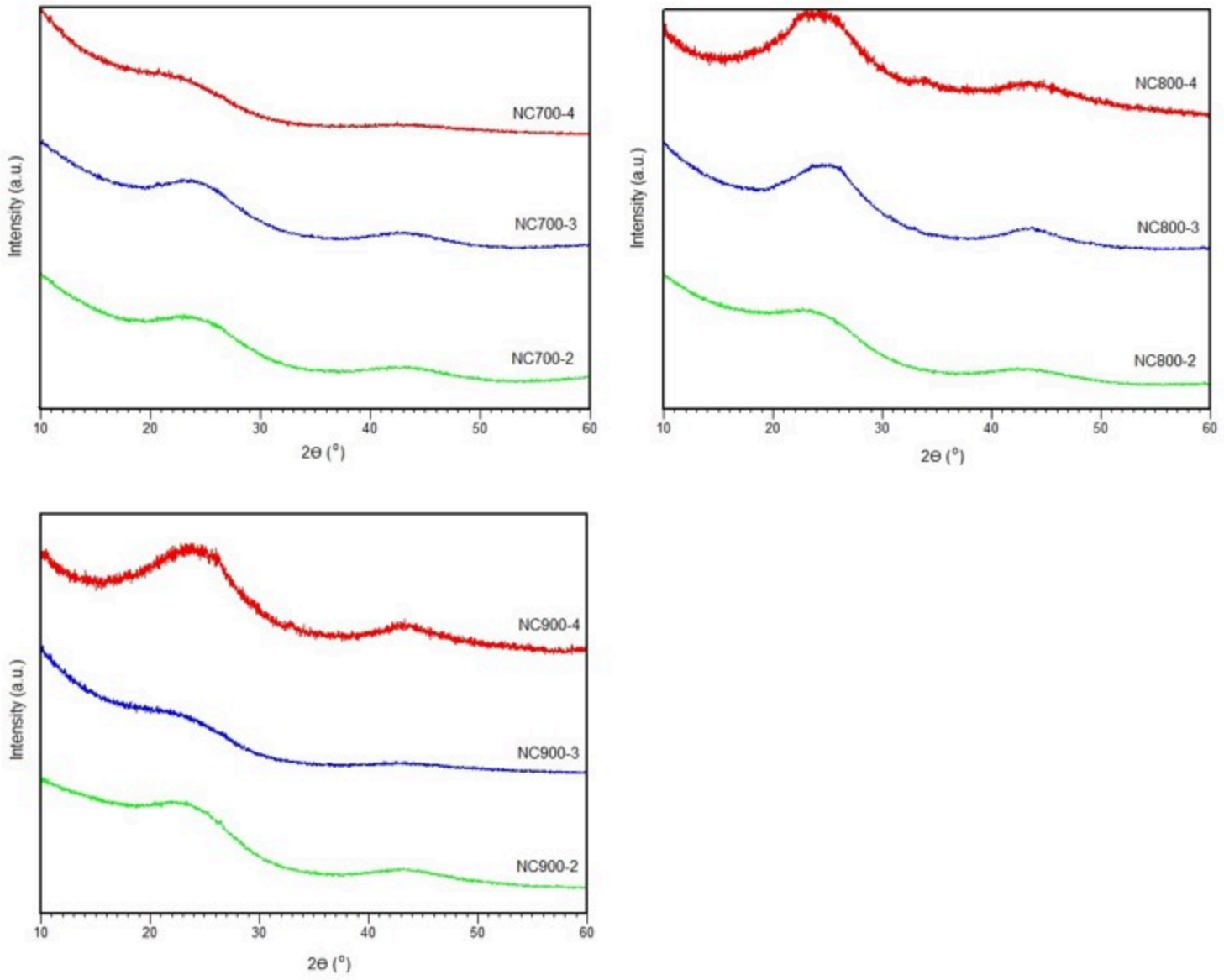

Figure 1

XRD patterns of the nanoporous carbon prepared at different gas flows and temperatures

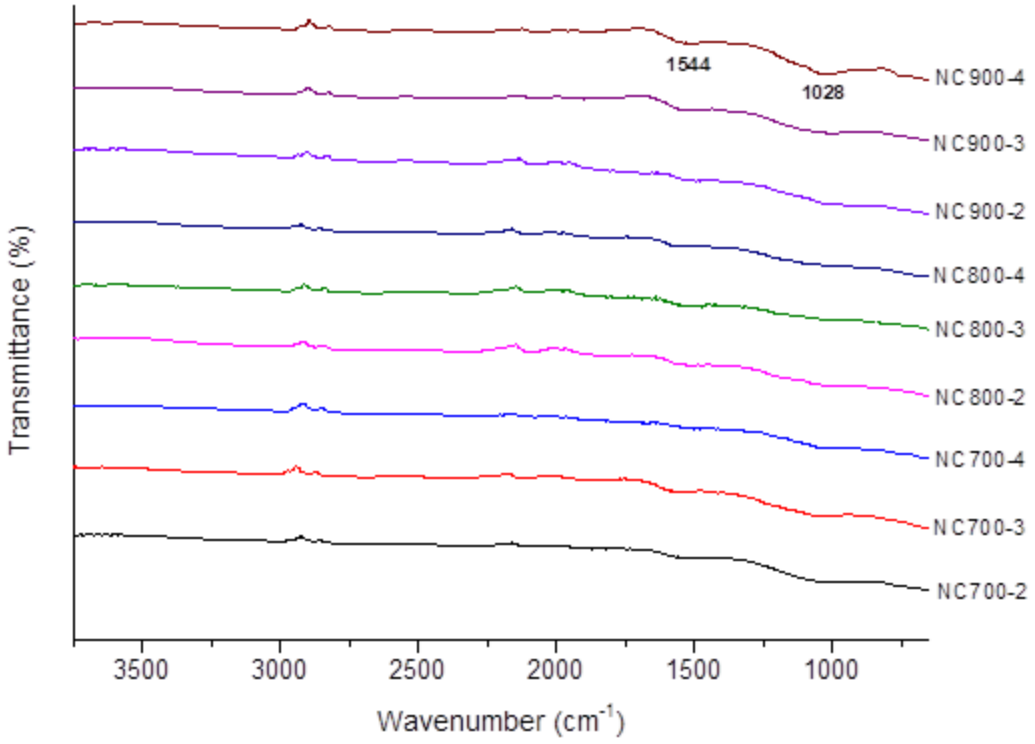

Figure 2

ATR-FTIR spectra of the nanoporous carbon derived from U. Lactuca

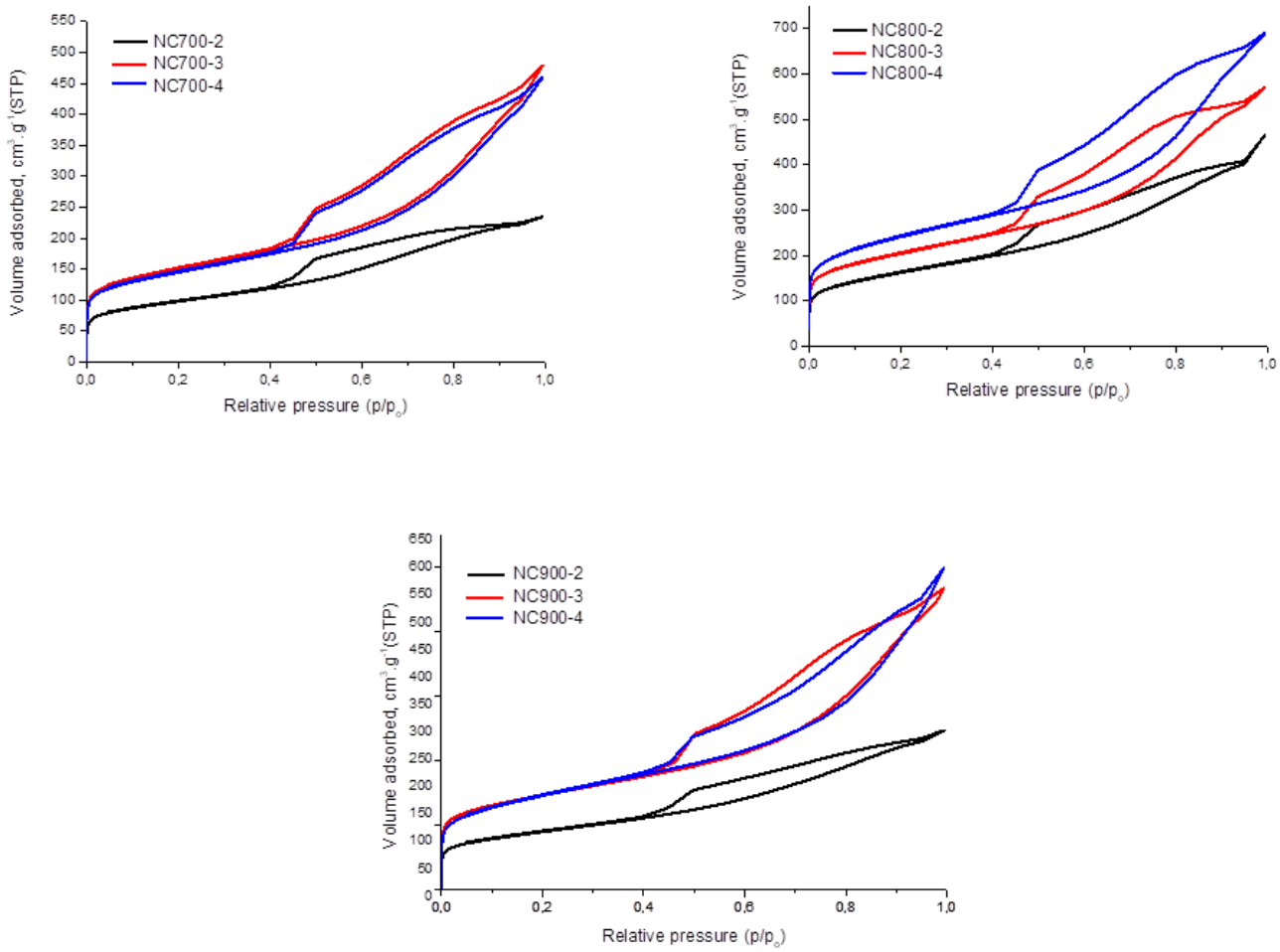

Figure 3

N_2 adsorption-desorption isotherms of nanoporous carbon from U. Lactuca

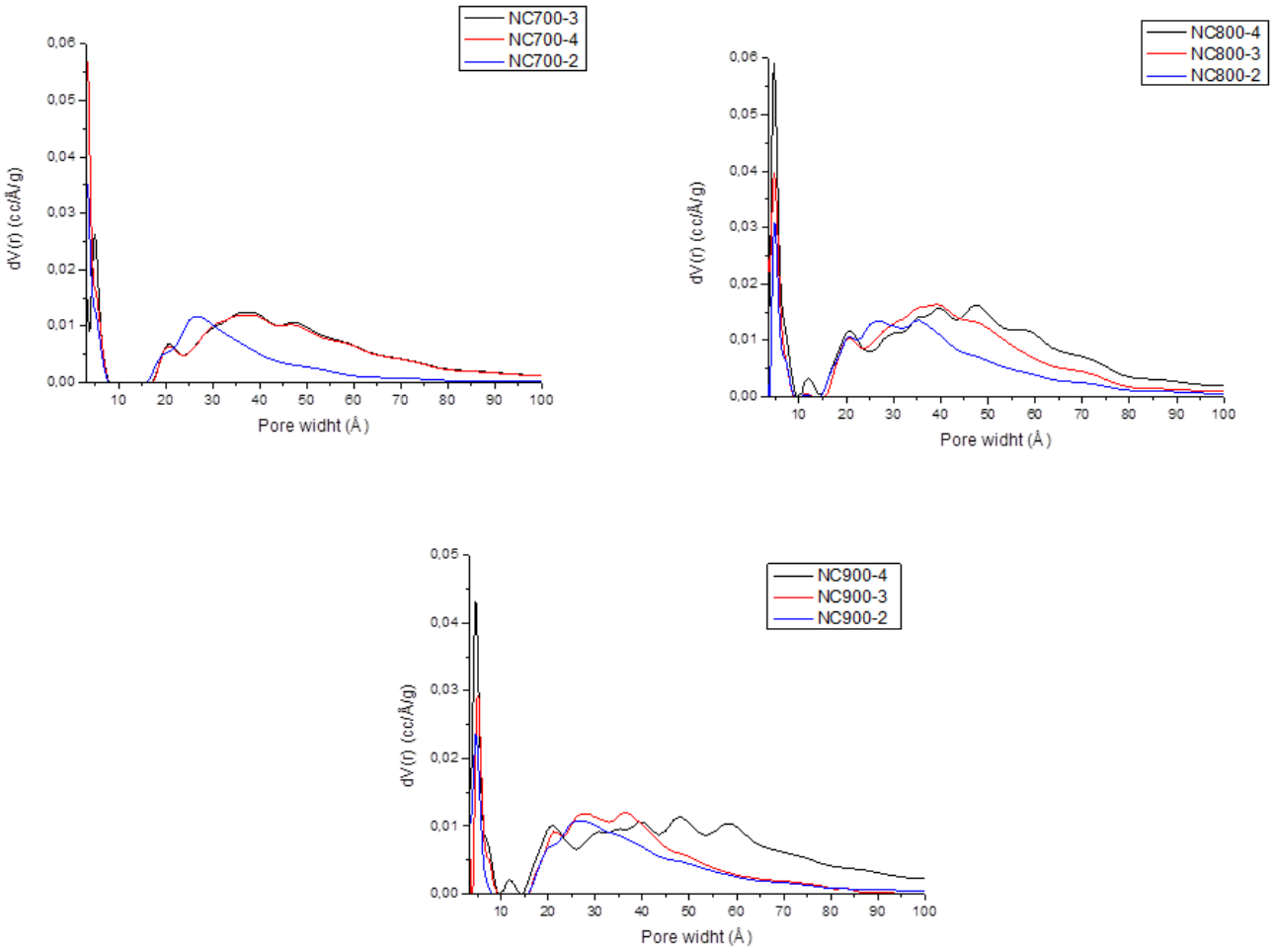

Figure 4

Pore size distribution graphs of samples prepared at different temperatures and flow rates

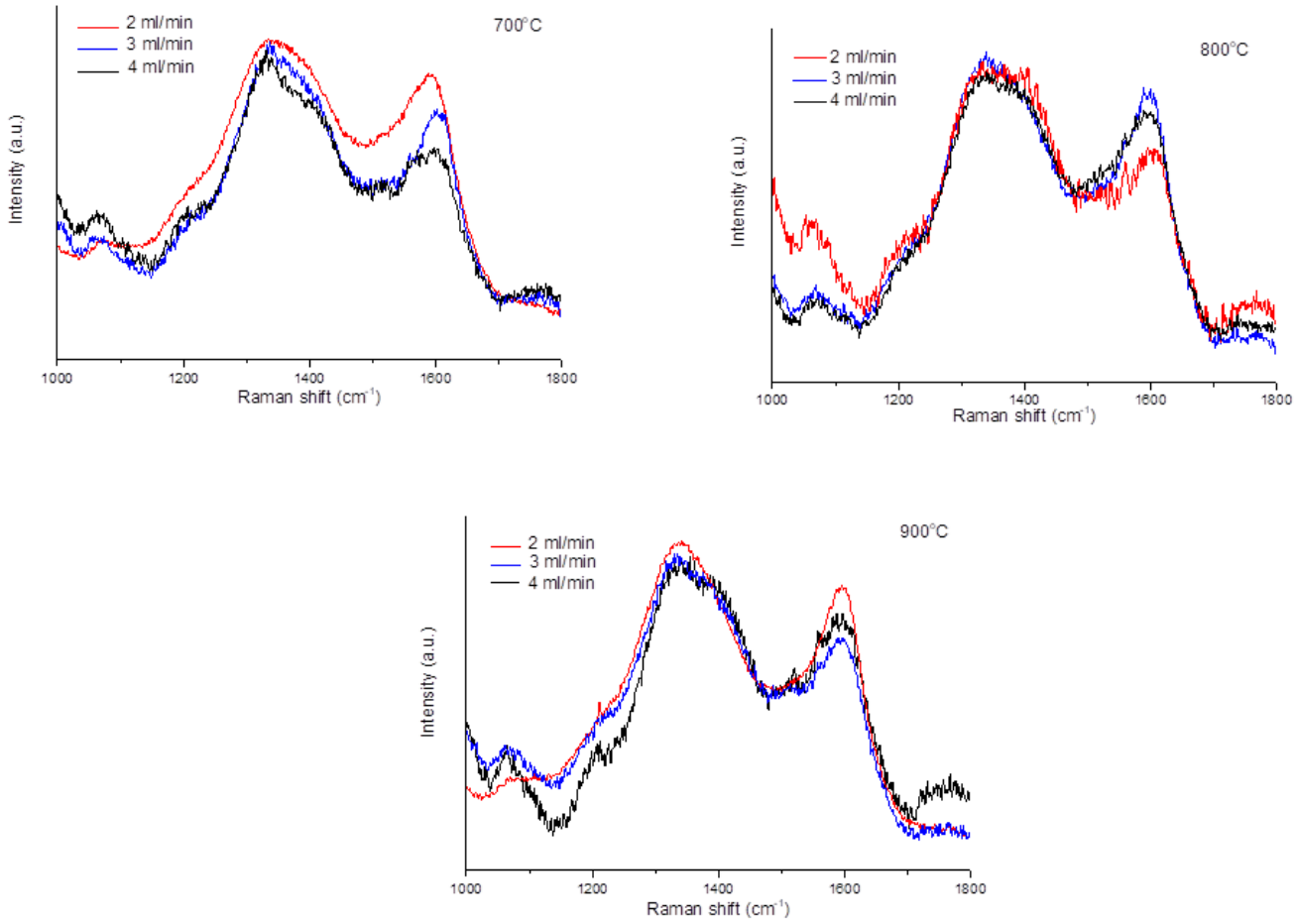

Figure 5

Raman spectra of the carbon samples prepared at different temperatures and flow rates

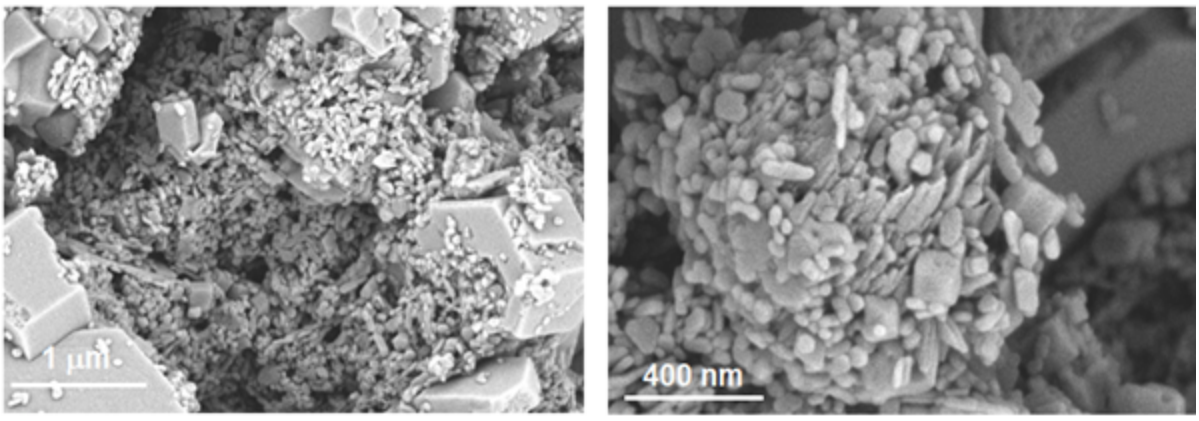

Figure 6

FE-SEM images of dried U. Lactuca and eggshell mixture at different magnifications

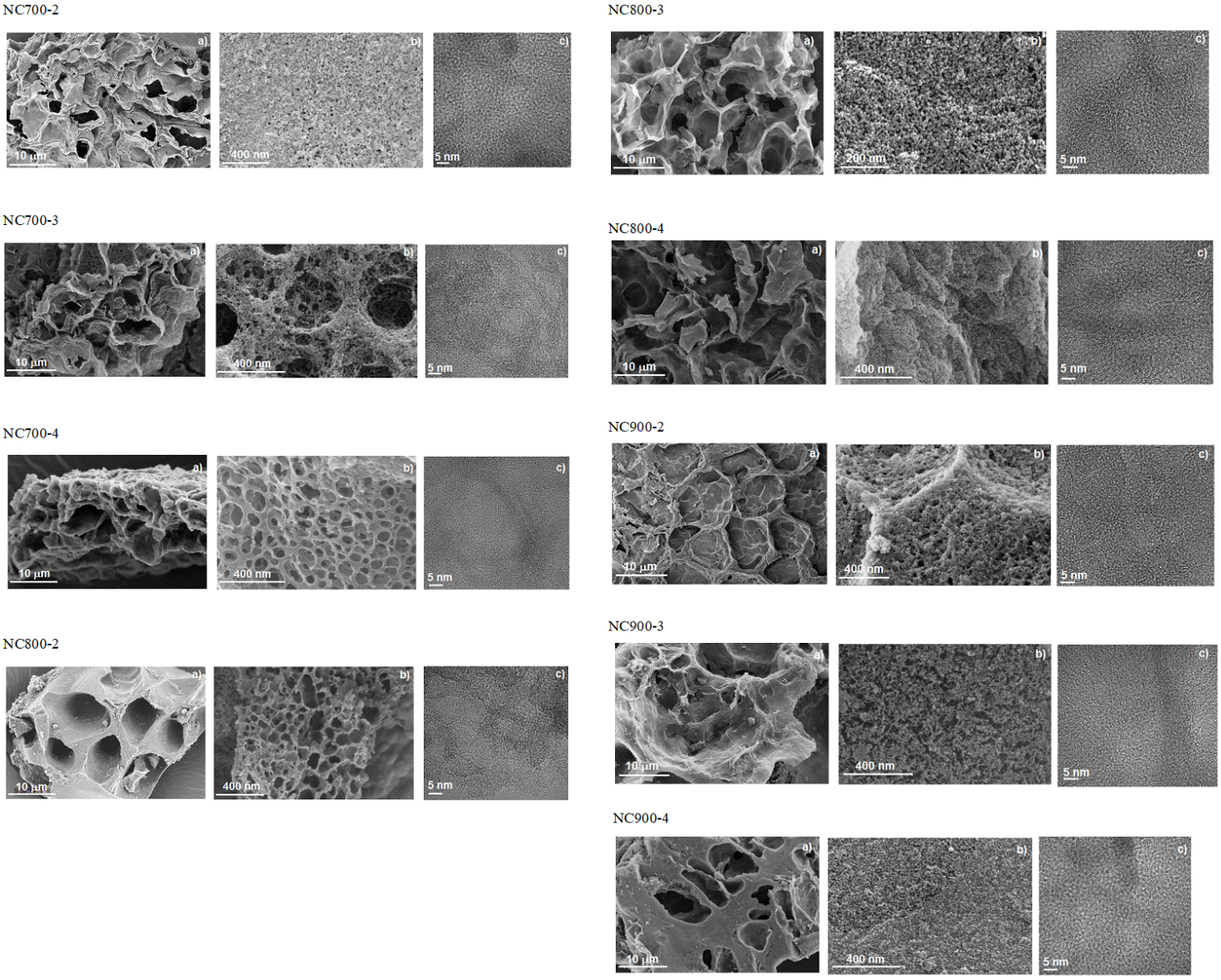

Figure 7

a), b) FE-SEM images at different magnifications and c) TEM images of nanoporous carbons

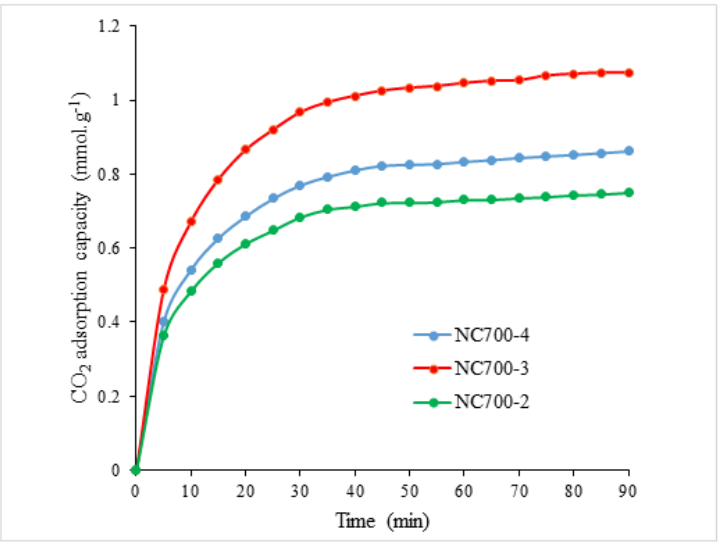

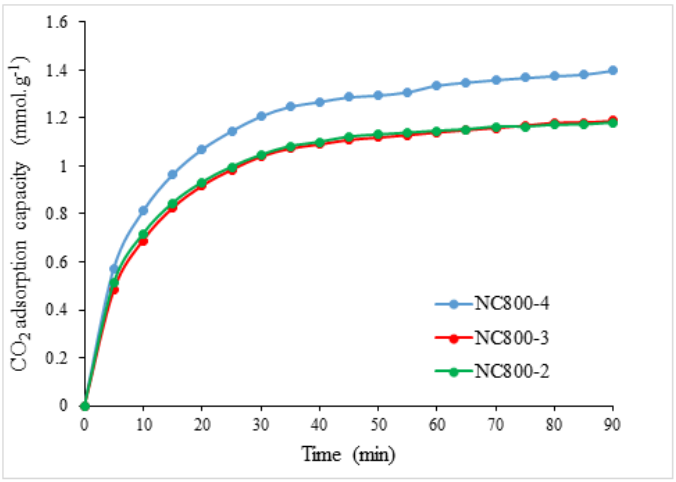

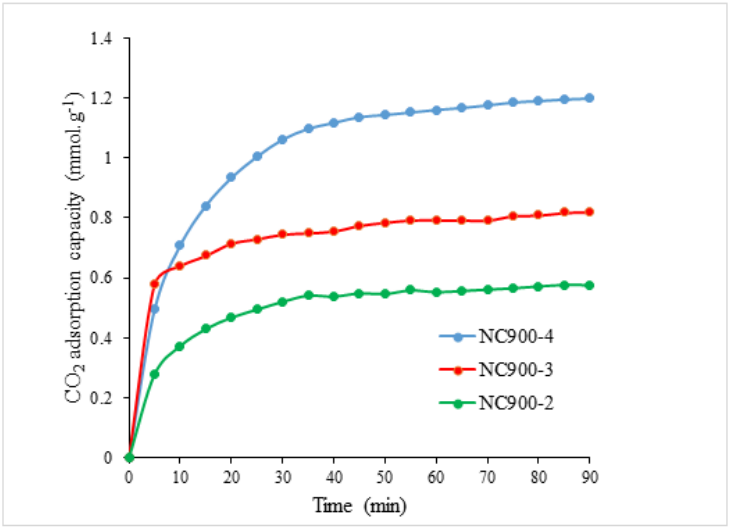

Figure 8

Change of CO_2 capture capacities of nanoporous carbons at 30°C over time.

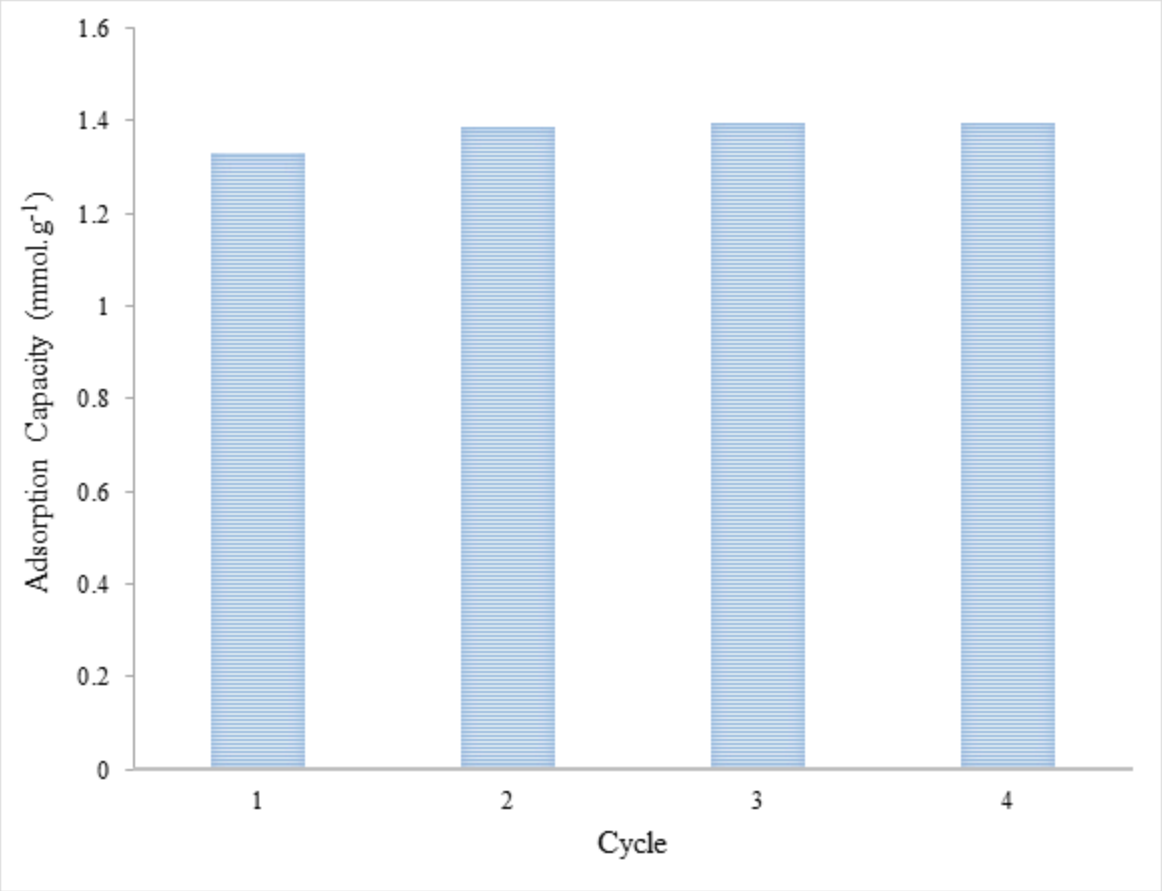

Figure 9

Adsorption/desorption cycle of NC800-4 at 30°C.

Supplementary Files

This is a list of supplementary files associated with this preprint. Click to download.

- GraphicalAbstracts.docx